

A new class of collective excitations of the Hubbard model I: η excitation of the negative- U model

Eugene Demler* and Shou-Cheng Zhang

Department of Physics, Stanford University, Stanford, CA 94305

Nejat Bulut and Douglas J. Scalapino

Department of Physics, UC at Santa Barbara, Santa Barbara, CA 93106

(May 7, 2019)

Abstract

In this series of papers we present a detailed study of the particle-particle collective excitations of the Hubbard model, and their contribution to the density and spin excitation spectrum. In the first paper, we shall investigate the singlet particle-particle pair with momentum (π, π) , the η particle, of the negative- U Hubbard model. We review three previously obtained theorems about the η particle and develop a self-consistent linear response theory which takes into account its contribution to the density excitation spectrum in the superconducting state. We show that this self-consistent theory agrees with the exact theorems as well as the results of numerical Monte Carlo simulations.

Typeset using REVTeX

*e-mail address: eugene@quantum.stanford.edu

I. INTRODUCTION

The Hubbard model provides a basic framework within which the nature of strongly-correlated electron systems have been studied. Recently, it was found that the Hubbard model has $SO(4)$ symmetry¹, for both positive and negative on-site Coulomb energy U . That is, besides the usual $SU(2)$ spin-rotation symmetry, it is also invariant under an $SU(2)$ “pseudo-spin” rotation group which contains the charge $U(1)$ symmetry as a subgroup. Based on this new symmetry, one of us^{2,3} derived a number of theorems and argued that this symmetry implies the existence of a collective excitation, the η -mode. This mode is characterized by a charge number of two, a spin quantum number zero, total momentum (π, π) and a sharp energy $U - 2\mu$. Here μ the chemical potential. As the momentum shifts away from (π, π) , the mode disperses and eventually merges into the continuum. Now, since this excitation has a charge quantum number of two, one can not couple to it in the normal state with the usual electric or magnetic-field probes¹ used to study the density and spin excitations of a many body system. However, if the system were to become superconducting, spontaneously breaking the $U(1)$ charge symmetry, then one should observe this η mode in the charge density response. Thus one has the unusual situation, that above T_c there is a well defined excitation in the many-body system which is invisible to the usual probes and it is only below T_c that we see this excitation.

Here we explore this phenomena for the negative- U Hubbard model. We begin with a review of the exact theorems regarding the η -mode. We then use a self-consistent linear response theory to approximately calculate correlations of the η and the charge density ρ in the superconducting state. We show that this approach gives results in agreement with the exact theorems and hence provides a meaningful approximation. Finally, we carry out Monte Carlo simulations for the two-dimensional negative- U Hubbard model and compare these with the approximate solution. In the Monte Carlo case, we can calculate the η - η correlation function above the Kosterlitz-Thouless temperature and clearly see the sharp η -mode in the normal state in this correlation function. We can then calculate the ρ - ρ charge density response and see that the η -mode becomes visible in the charge density response when the temperature is lowered and the pairing correlations extend over the lattice. We discuss these results and their possible relevance to other problems in the conclusions.

The formalism of self-consistent linear response theory takes into account the coupling of the particle-hole excitation and particle-particle excitation in the superconducting state. Such a formalism was first developed in the context of gauge invariance problem in superconductivity⁴⁻⁶. It was later used by Bardasis and Schrieffer^{7,8} to discuss the possibility of excitonic states inside the BCS energy gap. While the formalism we use here is similar to these previous works, the physical origin of the η mode is very different from the excitonic states inside the BCS energy gap. The excitonic states owe their existence to the BCS energy gap, they exist near a total momentum near zero, and disappear completely above T_c . The η mode, on the other hand, owes its existence to the collapse of the particle particle continuum near (π, π) and exists even in the normal state, although they decouple

¹In principle, a two-particle tunneling process could couple to this excitation but this would also require a superconductor.

from the density spectrum above T_c . After the prediction of the η mode in the Hubbard model², Kostyrko and Micnas⁹ have applied the conserving approximation in Nambu formalism to study the collective modes of the extended Hubbard model at zero temperature, and numerically confirmed the existence of the η mode in their formalism. In our present work we shall make the detailed comparison of $SO(4)$ Ward identities and the correlation functions derived using the self-consistent linear response theory, investigate the effect of finite temperature on the η mode, and demonstrate explicitly the scaling of its intensity with the superconducting order parameter.

Our present investigation is motivated in part by the recent neutron scattering experiments on the high T_c superconductors, in which a collective resonance was found below the superconducting transition temperature^{10–13}. This mode was interpreted by two of us¹⁴ as a triplet particle particle collective mode, hereafter called the π mode, of the positive U Hubbard model. Our motivation to study the details of the η mode of the negative U Hubbard model is to use it as a theoretical laboratory to verify a mechanism in which a particle particle collective mode can couple to the particle hole spectrum below the superconducting transition temperature, and to check the methodology used in the calculations. The η and π modes both have charge two and exist near momentum (π, π) , but they have different spin quantum numbers. The η mode has spin zero and energy of the order of $|U|$, while the π mode has spin one and energy of the order of J , the spin exchange energy. The similarities and the differences of these two collective modes will be addressed in detail in our next paper.

II. REVIEW OF THREE EXACT THEOREMS

In this section we shall review three main theorems of the Hubbard model derived by one of us in references^{2,3}. These results follow from Yang's work¹⁵ on the η pairing, and the $SO(4)$ symmetry of the Hubbard model¹. However, it is important to point out a physical difference between the following discussion and the idea of η pairing. While the idea of η pairing^{16,15} refers to a ground state property of the model, the following discussion assumes a conventional, zero total momentum pairing in the ground state, and the η pair is considered as an excitation of the system.

Let us start with the Hubbard Hamiltonian defined by

$$\mathcal{H} = -t \sum_{\langle ij \rangle} c_{i\sigma}^\dagger c_{j\sigma} + U \sum_i n_{i\uparrow} n_{i\downarrow} - \mu \sum_i c_{i\sigma}^\dagger c_{i\sigma} \quad (1)$$

Within this model, one can define the following operators

$$\begin{aligned} \eta^\dagger &= \sum_p c_{p+Q\uparrow}^\dagger c_{-p\downarrow}^\dagger \\ \eta &= (\eta^\dagger)^\dagger \\ \eta_0 &= \frac{1}{2}(N_e - N) \end{aligned} \quad (2)$$

where $Q = (\pi, \pi)$, N_e is the total number of electrons and N is the total number of lattice sites. It is easy to see that they form an $SU(2)$ algebra, called the pseudospin algebra:

$$[\eta_0, \eta^\dagger] = \eta^\dagger, \quad [\eta_0, \eta] = -\eta, \quad [\eta^\dagger, \eta] = 2\eta_0 \quad (3)$$

These η operators have a remarkable commutation property with the Hubbard Hamiltonian

$$[H, \eta^\dagger] = (U - 2\mu)\eta^\dagger, \quad [H, \eta_0] = 0, \quad [H, \eta^2] = 0 \quad (4)$$

Since the Hubbard Hamiltonian commutes with the Casimir operators η_0 and $\eta^2 \equiv \frac{1}{2}(\eta^\dagger\eta + \eta\eta^\dagger) + \eta_0\eta_0$ of the pseudospin algebra, the Hubbard Hamiltonian posses an $SO(4) = SU(2)_{spin} \times SU(2)_{pseudospin}$ symmetry group. These commutation rules and the symmetry property can be used to derive the following three important theorems, initially obtained in^{2,3}.

First let us consider the pure particle-particle correlation function involving only the η operators:

$$\begin{aligned} P(q, \omega) &= -i \int dt e^{i\omega t} \langle T \eta_q(t) \eta_q^\dagger(0) \rangle \\ &= \sum_n \left\{ \frac{|\langle n | \eta_q^\dagger | 0 \rangle|^2}{\omega - E_{n0} + i0} - \frac{|\langle n | \eta_q | 0 \rangle|^2}{\omega + E_{n0} - i0} \right\} \end{aligned} \quad (5)$$

where $\eta_q^\dagger = \sum_p c_{p+q\uparrow}^\dagger c_{-p\downarrow}^\dagger$ and the summation in the second line is over all the excited states $|n\rangle$.

For the case of $q = Q$, the operator η_q reduces to the η operator defined above. Throughout this paper we shall assume without loss of generality that system is less than half-filled, i.e. $N_e < N$. From the commutation relation with the Hubbard Hamiltonian, it is simple to see that η^\dagger operator creates a single excited state when acting on the ground state,²

$$|\eta\rangle = (1 - n)^{-\frac{1}{2}} \eta^\dagger |0\rangle \quad (6)$$

where a normalization factor is introduced such that

$$\begin{aligned} \langle \eta | \eta \rangle &= (1 - n)^{-1} \langle 0 | \eta \eta^\dagger | 0 \rangle = (1 - n)^{-1} \langle 0 | [\eta, \eta^\dagger] | 0 \rangle \\ &= (1 - n)^{-1} \sum_p (1 - n_{p\downarrow} - n_{p+Q\uparrow}) = 1 \end{aligned} \quad (7)$$

It is also easy to show that η annihilates the vacuum: $\eta|0\rangle = 0$ (we have already used this fact in (7) to replace the product of η and η^\dagger by their commutator).

Therefore only one term survives in (5) with $\langle n | = \langle \eta |$. And for $P(Q, \omega)$ we have

$$P(Q, \omega) = \frac{1}{(1 - n)} \frac{|\langle 0 | \eta \eta^\dagger | 0 \rangle|^2}{\omega - \omega_0 + i0} = \frac{(1 - n)}{\omega - \omega_0 + i0} \quad (8)$$

² In the consequent formulas we will be using the filling factor $n = N_e/N$ rather than N_e and will be omitting all the factors of N for brevity. So, that summation over all momenta p in our notations gives 1 and not N . This may be viewed as analog of normilization by a unit volume in the continious case. When needed the explicit dependence on N may be easily recovered.

where $\omega_0 = U - 2\mu$ is the energy of the η -particle. Equation (8) is the content of our first theorem.

Next let us consider a mixed correlation function involving the η operator and the density operator $\rho_q = \sum_{k\sigma} c_{k+q\sigma}^\dagger c_{k\sigma}$,

$$\begin{aligned} M(q, \omega) &= -i \int dt e^{i\omega t} \langle T \rho_{-q}(t) \eta_q^\dagger(0) \rangle \\ &= \sum_n \left\{ \frac{\langle 0 | \rho_{-q} | n \rangle \langle n | \eta_q^\dagger | 0 \rangle}{\omega - E_{n0} + i0} - \frac{\langle 0 | \eta_q^\dagger | n \rangle \langle n | \rho_{-q} | 0 \rangle}{\omega + E_{n0} - i0} \right\} \end{aligned} \quad (9)$$

For $q = Q$ we have contribution from the $|\eta\rangle$ -state only, and $M(Q, \omega)$ becomes

$$M(Q, \omega) = \frac{\langle 0 | \rho_{-Q} \eta_Q^\dagger | 0 \rangle}{(1-n)} \frac{1}{\omega - \omega_0 + i0} = -2 \frac{\langle \Delta \rangle}{U(1-n)} \frac{1}{\omega - \omega_0 + i0} \quad (10)$$

where $\Delta = -U \sum_k c_{k\uparrow}^\dagger c_{-k\downarrow}^\dagger$ is the superconducting order parameter. Equation (10) is our second theorem.

Finally, let us consider the pure density-density correlation function defined by

$$\begin{aligned} D(q, \omega) &= -i \int dt e^{i\omega t} \langle T \rho_{-q}(t) \rho_q(0) \rangle \\ &= \sum_n |\langle 0 | \rho_{-q} | n \rangle|^2 \left\{ \frac{1}{\omega - E_n + i0} - \frac{1}{\omega + E_n - i0} \right\} \end{aligned} \quad (11)$$

For $D(Q, \omega)$ we can pull out the part singular at ω_0

$$\begin{aligned} D(Q, \omega) &= \frac{|\langle 0 | \rho_{-Q} | \eta \rangle|^2}{\omega - \omega_0 + i0} + \text{part regular at } \omega_0 \\ &= (1-n)^{-1} \frac{|\langle 0 | [\rho_{-Q}, \eta^\dagger] | 0 \rangle|^2}{\omega - \omega_0 + i0} + \text{part regular at } \omega_0 \\ &= 4 \frac{\langle \Delta \rangle^2}{U^2(1-n)} \frac{1}{\omega - \omega_0 + i0} + \text{part regular at } \omega_0 \end{aligned} \quad (12)$$

Equation (12) is our third theorem.

From expressions (8), (10) and (12) we can see that all the correlation functions have poles at ω_0 and their residues are expressed as simple combinations of parameters of the system. We want to emphasize again that these three results are exact and do not require any approximations in their derivations, and they are valid for both the positive and the negative U Hubbard model.

Among all three of these theorems, the third one is the most interesting, since the density correlation function can be measured directly in experiments. This theorem predicts that a new collective excitation, the η particle can be found in the density spectrum, whose intensity is directly proportional to the square of the superconducting order parameter, in this case, an s -wave order parameter. Physically this is because the density correlation function measures a particle hole like excitation, and therefore, the η particle, which has charge two rather than zero, can only make a finite contribution if the quasi-particle excitations are

a coherent admixture of particles and holes. The mixing amplitude is exactly proportional to the square of the superconducting order parameter. For a momentum $Q = (\pi, \pi)$ the energy of the η -mode is $\omega_0 = U - 2\mu$. However, unlike the first two theorems, the third theorem only makes a partial prediction about a correlation function, namely the part that is singular at ω_0 . For this reason, it is highly desirable to find an approximate scheme which yields complete information about the full momentum and frequency range of the density correlation function, and reduces to the exact theorem for the special momentum Q and frequency ω_0 . Such an investigation is carried out in the subsequent sections.

III. SELF-CONSISTENT LINEAR RESPONSE THEORY

A. Formalism

In calculating the density response in the superconducting state, it is known that one must take into account the collective motion of the condensate in a self-consistent manner as well as the usual quasi-particle-hole excitations. An externally applied density disturbance ϕ_q at wave length q generates two kinds of responses in the system, single-particle like excitations across the energy gap, and a collective motion of the condensate expressed as a pairing amplitude η_q , and a density field ρ_q , at a finite wave length q . The usual RPA formula in the superconducting state takes into account the self-consistent density field ρ_q , but does not treat the self-consistent pairing field η_q . As we shall show, such an approximation is not fully self-consistent and violates the $SO(4)$ symmetry of the Hubbard model. On the other hand, a fully self-consistent treatment of both the density and the pairing field correctly describes the contribution of the η particle in the superconducting state, and reduces to the exact theorems reviewed in the previous section.

In the following, we review the basic formalism. In the Appendix we compare our results to the formulas one gets from the equations of motion method and from the diagrammatical approach. In both cases we find exact agreement.

Our starting point is the negative- U Hubbard Hamiltonian perturbed by an infinitesimally small external field ϕ_q which is coupled to the $-q$ component of the density.

$$\mathcal{H} = -t \sum_{\langle ij \rangle} c_{i\sigma}^\dagger c_{j\sigma} + U \sum_i n_{i\uparrow} n_{i\downarrow} - \mu \sum_i c_{i\sigma}^\dagger c_{i\sigma} + \frac{1}{2} U \rho_{-q} \phi_q \quad (13)$$

We will assume that our system is in a superconducting ground state characterized by the nonvanishing averages of the zero momentum operators

$$\begin{aligned} \langle c_{k\sigma}^\dagger c_{k\sigma} \rangle &= v_k^2 \\ \langle c_{-k\downarrow} c_{k\uparrow} \rangle &= \langle c_{k\uparrow}^\dagger c_{-k\downarrow}^\dagger \rangle = u_k v_k. \end{aligned} \quad (14)$$

Here the parameters u_k and v_k are given by

$$u_k^2 = \frac{1}{2} \left(1 + \frac{\epsilon_k}{E_k} \right) \quad (15)$$

$$v_k^2 = \frac{1}{2} \left(1 - \frac{\epsilon_k}{E_k} \right) \quad (16)$$

with $\epsilon_k = -2t(\cos k_x + \cos k_y) - \mu$, $E_k = \sqrt{\epsilon_k^2 + \Delta^2}$ and the BCS self-consistency condition is implied

$$\Delta = -U \sum_p u_p v_p \quad (17)$$

After we turn on the perturbation, the operators in (14) are no longer the only operators with nonvanishing expectation values. The expectation values of the following operators carrying momentum q are induced as well.

$$\begin{aligned} \langle \eta_q^\dagger(t) \rangle &= \sum_k \langle c_{k+q\uparrow}^\dagger(t) c_{-k\downarrow}^\dagger(t) \rangle \\ \langle \eta_q(t) \rangle &= \sum_k \langle c_{-k-q\downarrow}(t) c_{k\uparrow}(t) \rangle \\ \langle \rho_{q\uparrow}(t) \rangle &= \sum_k \langle c_{k+q\uparrow}^\dagger(t) c_{k\uparrow}(t) \rangle \\ \langle \rho_{q\downarrow}(t) \rangle &= \sum_k \langle c_{-k\downarrow}^\dagger(t) c_{-k-q\downarrow}(t) \rangle \end{aligned} \quad (18)$$

The operators in (18) describe the collective motion of the superconducting condensate. Within the self-consistent linear response theory, the local operators respond to the local field, which is the sum of the external disturbance ϕ_q and the induced self-consistent field given in equation (18). It is very important that in (18) we take into account not only the particle-hole channel as is usually done in RPA but also the particle-particle and hole-hole channels.

The Hamiltonian (13) can be linearized with respect to the usual BCS pairing fields and the induced fields (18) giving ³ :

$$\begin{aligned} \mathcal{H} &= \sum_{p\sigma} \epsilon_p c_{p\sigma}^\dagger c_{p\sigma} + \Delta c_{p\uparrow}^\dagger c_{-p\downarrow}^\dagger + \Delta c_{-p\downarrow} c_{p\uparrow} \\ &+ U \eta_q^* \sum_{k'} c_{-k'\downarrow} c_{k'+q\uparrow} + U \eta_q \sum_{k'} c_{k'-q\uparrow}^\dagger c_{-k'\downarrow}^\dagger \\ &+ U(\rho_{q\uparrow} + \frac{\phi_q}{2}) \sum_{k'} c_{k'-q\downarrow}^\dagger c_{k'\downarrow} + U(\rho_{q\downarrow} + \frac{\phi_q}{2}) \sum_{k'} c_{k'-q\uparrow}^\dagger c_{k'\uparrow} \end{aligned} \quad (19)$$

The first line in the last equation will be considered as an unperturbed Hamiltonian \mathcal{H}_0 . Since the fields in (18) are proportional to ϕ_q one can use the Kubo formula and treat the last four terms in (19) as a perturbation \mathcal{H}_1 . Thus the response $\langle \hat{f}(t) \rangle$ is given by

$$\langle \hat{f}(t) \rangle = -i \int_{-\infty}^t dt' \langle [\hat{f}(t), \mathcal{H}_1(t')] \rangle_{\mathcal{H}_0}, \quad (20)$$

and f can be any of the operators η_q^\dagger , η_q , $\rho_{q\uparrow}$ or $\rho_{q\downarrow}$. When combined, these equations form a self-consistent set of equations and the expectation values in equation (18) can be solved

³ To prevent any possible confusion we want to clarify that in this Section η_q , $\rho_{q\uparrow\downarrow}$ and $\eta_q^* = \langle \eta_q^\dagger \rangle$ are the *expectation values* of the corresponding operators and in commutation relations must be considered as c-numbers.

for purely in terms of the external field ϕ_q . As an example of how one can proceed from (20) we will show explicitly the calculations for η_q^* .

$$\begin{aligned}
\eta_q^*(t) = & -i \sum_k \int_{-\infty}^t dt' \langle [c_{k+q\uparrow}^\dagger(t) c_{-k\downarrow}^\dagger(t), \mathcal{H}_1(t')] \rangle_{\mathcal{H}_0} = \\
& -iU \int_{-\infty}^t \eta_q^*(t') dt' \sum_{kk'} \langle [c_{k+q\uparrow}^\dagger(t) c_{-k\downarrow}^\dagger(t), c_{-k'\downarrow}(t') c_{k'+q\uparrow}(t')] \rangle_{\mathcal{H}_0} \\
& -iU \int_{-\infty}^t \eta_q(t') dt' \sum_{kk'} \langle [c_{k+q\uparrow}^\dagger(t) c_{-k\downarrow}^\dagger(t), c_{k'-q\uparrow}^\dagger(t') c_{-k'\downarrow}^\dagger(t')] \rangle_{\mathcal{H}_0} \\
& -iU \int_{-\infty}^t (\rho_{q\uparrow}(t') + \frac{1}{2}\phi_q(t')) dt' \sum_{kk'} \langle [c_{k+q\uparrow}^\dagger(t) c_{-k\downarrow}^\dagger(t), c_{k'-q\downarrow}^\dagger(t') c_{k'\downarrow}(t')] \rangle_{\mathcal{H}_0} \\
& -iU \int_{-\infty}^t (\rho_{q\downarrow}(t') + \frac{1}{2}\phi_q(t')) dt' \sum_{kk'} \langle [c_{k+q\uparrow}^\dagger(t) c_{-k\downarrow}^\dagger(t), c_{k'-q\uparrow}^\dagger(t') c_{k'\uparrow}(t')] \rangle_{\mathcal{H}_0} \quad (21)
\end{aligned}$$

When we perform a Fourier transform of the last equation it is helpful to make use of the usual trick of replacing the commutator with a time-ordered Green's function and shifting the poles to the lower-half plane at the end. This will give us the following expression for $\eta_{q\omega} \equiv \int dt \eta_q(t) e^{i\omega t}$ (Fourier components of the other functions are defined analogously)

$$\begin{aligned}
\eta_{q\omega}^* = & iU \sum_p \int \frac{d\nu}{2\pi} G_p(\nu) G_{p+q}(-\nu - \omega) \eta_{q\omega}^* \\
& -iU \sum_p \int \frac{d\nu}{2\pi} F_p^*(\nu) F_{p+q}^*(\nu + \omega) \eta_{q\omega} \\
& -iU \sum_p \int \frac{d\nu}{2\pi} F_p^*(\nu) G_{p+q}(\nu - \omega) (\rho_{q\omega} + \phi_{q\omega}) \quad (22)
\end{aligned}$$

where we introduced $\rho_{q\omega} = \rho_{q\omega\downarrow} + \rho_{q\omega\uparrow}$, and $G_p(\omega) \equiv \int e^{i\omega t} (-i) \langle T c_{p\sigma}(t) c_{p\sigma}^\dagger(0) \rangle dt$ and $F_p(\omega) \equiv \int e^{i\omega t} (-i) \langle T c_{p\uparrow}(t) c_{-p\downarrow}(0) \rangle dt$ are the usual BCS Greens functions. We remind the reader that after performing the frequency integration in (22) one should shift all the poles of the final expression to the lower half-plane. Similar expressions can be easily obtained for $\eta_{q\omega}$ and $\rho_{q\omega}$.

$$\begin{aligned}
\eta_{q\omega} = & -iU \sum_p \int \frac{d\nu}{2\pi} F_p(\nu) F_{p+q}(\nu + \omega) \eta_{q\omega}^* \\
& +iU \sum_p \int \frac{d\nu}{2\pi} G_p(\nu) G_{p+q}(\omega - \nu) \eta_{q\omega} \\
& -iU \sum_p \int \frac{d\nu}{2\pi} F_p(\nu) G_{p+q}(\nu + \omega) (\rho_{q\omega} + \phi_{q\omega}) \quad (23)
\end{aligned}$$

$$\begin{aligned}
\rho_{q\omega} = & -iU \sum_p \int \frac{d\nu}{2\pi} F_{p+q}(\nu) G_p(\nu - \omega) \eta_{q\omega}^* \\
& -iU \sum_p \int \frac{d\nu}{2\pi} F_{p+q}^*(\nu) G_p(\nu + \omega) \eta_{q\omega} \\
& +iU \sum_p \int \frac{d\nu}{2\pi} \{ F_p(\nu) F_{p+q}(\nu + \omega) - G_p(\nu) G_{p+q}(\nu + \omega) \} (\rho_{q\omega} + \phi_{q\omega}) \quad (24)
\end{aligned}$$

In the diagrammatic language these equations correspond to the vertex corrections for scattering in the particle-particle, particle-hole and hole-hole channels and are presented in Appendix B. Generalization of formulas (22) - (24) to the case of finite temperatures can be accomplished by substituting $i \int \frac{d\nu}{2\pi} \rightarrow -T \sum_{\nu_n}$. Skipping laborious but straightforward calculations we present the final expressions leaving their derivation aside. We introduce the matrix equation

$$\begin{pmatrix} \eta_{q\omega}^* + \eta_{q\omega} \\ \eta_{q\omega}^* - \eta_{q\omega} \\ \rho_{q\omega}^\dagger \end{pmatrix} = \begin{vmatrix} t_{++} & t_{+-} & m_+ \\ t_{+-} & t_{--} & m_- \\ m_+ & m_- & -U\chi_{bcs} \end{vmatrix} \begin{pmatrix} \eta_{q\omega}^* + \eta_{q\omega} \\ \eta_{q\omega}^* - \eta_{q\omega} \\ \rho_{q\omega} + \phi_{q\omega} \end{pmatrix} \quad (25)$$

where the matrix elements are given by the following expressions,

$$\begin{aligned} t_{++} = & U \sum_p [1 - f(E_{p+q}) - f(E_p)] \frac{\Omega_{pq}(1 - v_{p+q}^2 - v_p^2)}{\omega^2 - \nu_{pq}^2 + i0} \\ & + U [f(E_{p+q}) - f(E_p)] \frac{(E_{p+q} - E_p)(u_p v_{p+q} + v_p u_{p+q})^2}{\omega^2 - \theta_{pq}^2 + i0} \end{aligned} \quad (26)$$

$$\begin{aligned} t_{+-} = & -U \sum_p [1 - f(E_{p+q}) - f(E_p)] \frac{\omega(1 - v_{p+q}^2 - v_p^2)}{\omega^2 - \nu_{pq}^2 + i0} \\ & - U [f(E_{p+q}) - f(E_p)] \frac{\omega(v_{p+q}^2 - v_p^2)}{\omega^2 - \theta_{pq}^2 + i0} \end{aligned} \quad (27)$$

$$\begin{aligned} t_{--} = & U \sum_p [1 - f(E_{p+q}) - f(E_p)] \frac{\nu_{pq}(u_{p+q}u_p + v_{p+q}v_p)^2}{\omega^2 - \nu_{pq}^2 + i0} \\ & + U [f(E_{p+q}) - f(E_p)] \frac{\theta_{pq}(u_p v_{p+q} - v_p u_{p+q})^2}{\omega^2 - \theta_{pq}^2 + i0} \end{aligned} \quad (28)$$

$$\begin{aligned} m_+ = & U \sum_p [1 - f(E_{p+q}) - f(E_p)] \frac{\Omega_{pq}(u_p v_p + u_{p+q} v_{p+q})}{\omega^2 - \nu_{pq}^2 + i0} \\ & - U [f(E_{p+q}) - f(E_p)] \frac{\Omega_{pq}(u_{p+q} v_{p+q} - u_p v_p)}{\omega^2 - \theta_{pq}^2 + i0} \end{aligned} \quad (29)$$

$$\begin{aligned} m_- = & -U \sum_p [1 - f(E_{p+q}) - f(E_p)] \frac{\omega(u_p v_p + u_{p+q} v_{p+q})}{\omega^2 - \nu_{pq}^2 + i0} \\ & + U [f(E_{p+q}) - f(E_p)] \frac{\omega(u_{p+q} v_{p+q} - u_p v_p)}{\omega^2 - \theta_{pq}^2 + i0} \end{aligned} \quad (30)$$

$$\begin{aligned} \chi_{bcs} = & - \sum_p [1 - f(E_{p+q}) - f(E_p)] \frac{\nu_{pq}(u_{p+q}v_p + v_{p+q}u_p)^2}{\omega^2 - \nu_{pq}^2 + i0} \\ & + [f(E_{p+q}) - f(E_p)] \frac{\theta_{pq}(u_p u_{p+q} - v_p v_{p+q})^2}{\omega^2 - \theta_{pq}^2 + i0} \end{aligned} \quad (31)$$

In the equations above $\omega_{pq} = \epsilon_{p+q} - \epsilon_p$, $\Omega_{pq} = \epsilon_{p+q} + \epsilon_p$, $\nu_{pq} = E_{p+q} + E_p$, $\theta_{pq} = E_{p+q} - E_p$ and $f(E)$ is the Fermi distribution function.

Solution of the density part of the matrix equation (25) can be written in a very suggestive form:

$$\rho_{q\omega} = \frac{-U\chi_{bcs} + \frac{m_+^2 + m_-^2 - m_-^2 t_{++} + 2m_+ m_- t_{+-} - m_+^2 t_{--}}{1 - t_{++} - t_{+-}^2 - t_{--} + t_{++} t_{--}}}{1 + U\chi_{bcs} - \frac{m_+^2 + m_-^2 - m_-^2 t_{++} + 2m_+ m_- t_{+-} - m_+^2 t_{--}}{1 - t_{++} - t_{+-}^2 - t_{--} + t_{++} t_{--}}} \phi_{q\omega} \quad (32)$$

It is easy to see that the last terms in both the numerator and the denominator are proportional to the BCS pairing amplitude, therefore, this expression reduces to the usual RPA formula in the normal state. In the superconducting state however, these correction terms make important contributions, and it would be *incorrect* to neglect them. These terms take into account the self-consistent pairing fields in the superconducting state, and in the diagrammatic language, they arise from multiple scattering in the particle-particle and the hole-hole channels. Equation (32) agrees with the expression for the density-density correlation function derived by Kostyrko and Micnas⁹. Formulas (25) - (32) are the core of the Self-consistent Linear Response Theory. In Part B we will show analytically that for the case of $q = Q$ and $\omega = \omega_0$, these formulas reduce to the exact theorem given in the previous section, with the correct location of the poles and the residues. In Part C we compare these results with numerical calculations.

B. Comparisons with exact theorems

Here we show how our formulas (25) for $T = 0$ reduce to the exact results (10) and (12) for $Q = (\pi, \pi)$. This point has a property that $\Omega_{pQ} = -2\mu$ for all momenta p . Therefore Ω_{pQ} may be taken outside the p summation in the equations of (25) and a number of interesting identities arise.

We start by multiplying the first equation in (25) by ω , the second by Ω_{pq} and adding these two equations. After a few simple manipulations the resulting expression can be written as ⁴

$$\omega(\eta_{Q\omega}^* + \eta_{Q\omega}) = [-\Omega_{pQ} - U(1 - n)](\eta_{Q\omega}^* - \eta_{Q\omega}) \quad (33)$$

We can prove the following relationship $\nu_{pq}(v_p u_{p+q} + v_{p+q} u_p)^2 = \left[\frac{\nu_{pq}^2 - \omega^2}{2\Delta} + \frac{\omega^2 - \Omega_{pq}^2}{2\Delta} \right] (u_p v_p + u_{p+q} v_{p+q})$ and use it to write the third equation of (25) in the form

$$\begin{aligned} -2\Delta\phi_{q\omega} &= 2\Delta U \sum_p \frac{\Omega_{pq}(u_p v_p + u_{p+q} v_{p+q})}{\omega^2 - \nu_{pq}^2 + i0} (\eta_{q\omega}^* + \eta_{q\omega}) \\ &\quad - 2\Delta U \sum_p \frac{\omega(u_p v_p + u_{p+q} v_{p+q})}{\omega^2 - \nu_{pq}^2 + i0} (\eta_{q\omega}^* - \eta_{q\omega}) \\ &\quad + U \sum_p \frac{\omega^2 - \Omega_{pq}^2}{\omega^2 - \nu_{pq}^2 + i0} (u_p v_p + u_{p+q} v_{p+q}) (\rho_{q\omega} + \phi_{q\omega}) \end{aligned} \quad (34)$$

⁴ We remind the reader that since the present analysis is for $T = 0$, all the fermi functions in (26) - (31) vanish.

We add to (34) the first equation of (25) multiplied by Ω_{pQ} and the second multiplied by ω to obtain⁵

$$\omega(\eta_{Q\omega}^* - \eta_{Q\omega}) = [-\Omega_{pQ} - U(1 - n)](\eta_{Q\omega}^* + \eta_{Q\omega}) + 2\Delta\phi_Q \quad (35)$$

Equations (33) and (35) can be solved for $\eta_{Q\omega}^*$ and $\eta_{Q\omega}$ in terms of ϕ_Q

$$\eta_{Q\omega}^* = \frac{\Delta}{\omega + \omega_0}\phi_{Q\omega} \quad \eta_{Q\omega} = -\frac{\Delta}{\omega - \omega_0}\phi_{Q\omega} \quad (36)$$

where we introduced $\omega_0 = U(1 - n) + \Omega_{pQ} = U(1 - n) - 2\mu$.⁶ Now, the expressions (36) by themselves give us a mixed correlation function (9) or they can be inserted into any of the equations of (25) giving the density-density correlation function

$$M(Q, \omega) = \frac{\eta_{q\omega}}{\frac{U}{2}\phi_{q\omega}} = -\frac{2\Delta}{U} \frac{1}{\omega - \omega_0 + i0} \quad (37)$$

$$D(Q, \omega) = \frac{\rho_{q\omega}}{\frac{U}{2}\phi_{q\omega}} = -2 \frac{\chi_{bcs}(Q, \omega) + 2 \frac{\omega^2 - 2\mu\omega_0}{\omega^2 - \omega_0^2} \Delta I_2(Q, \omega)}{1 + U\chi_{bcs}(Q, \omega)} \quad (38)$$

where $I_2(Q, \omega) = \sum_p \frac{u_p v_p + u_{p+Q} v_{p+Q}}{\omega^2 - v_{pQ}^2}$. From (38) we immediately see that $D(Q, \omega)$ has a pole at $\omega = \omega_0$ corresponding to the η -pair and using

$$1 + U\chi_{bcs}(Q, \omega) = -\frac{U}{2\Delta}(\omega^2 - \Omega_{pQ}^2)I_2(Q, \omega) \quad (39)$$

we can write (38) as

$$D(Q, \omega) = 4 \frac{\Delta^2}{U^2(1 - n)} \frac{1}{\omega - \omega_0 + i0} + \text{part regular at } \omega_0 \quad (40)$$

Thus the Self-consistent Linear Response expressions agree with the exact theorems, giving the correct position of the resonance as well as the same values for the residues of all correlation functions. Here we have explicitly verified theorems 2 and 3 from last section. In order to verify theorem 1, one needs to add an external pairing disturbance, in addition

⁵ Equations (33) and (35) arise directly if one writes the equations of motion for $\sum_p(\eta_{pq}^* - \eta_{pq})$ and $\sum_p(\eta_{pq}^* + \eta_{pq})$

⁶ This expression may seem to give a different value for ω_0 than (4). This comes from the fact that in the Linear Response we do not take into account the Hatree-Fock corrections to the self-energy or in other words in the diagrams of Appendix C we do not consider corrections to the single particle Green's functions. In fact, the only effect of these corrections is to renormalize a chemical potential by an average effective field on each particle due to the interaction with the particles of opposite spin $\mu \rightarrow \mu - \frac{Un}{2}$. After such substitution this last expression for ω_0 is exactly the same as in (4). This procedure of Hartree-Fock corrections reducing to the renormalization of μ is explicit in the equations of motion.

to the density disturbance. Repeating the manipulations given above, it can be seen that theorem 1 is verified as well.

These results show that while the Self-consistent Linear Response Theory is still an approximate scheme, it is conserving in the sense that it respects the $SO(4)$ Wards identities expressed through theorems 1 to 3. On the other hand, a simple RPA expression in which one neglects the last terms in the numerator and the denominator of equation (32) violates the $SO(4)$ symmetry and is a poor approximate scheme.

C. Numerical results

Here we give numerical results for the spectral functions calculated from equation (32), with the full momentum, energy and temperature dependence. The calculations have been carried out for different U 's and n 's and the values of parameters are specified in the captions for each figure. The imaginary infinitesimal in the denominators was taken to be $\Gamma = 1.0 \times 10^{-2}$ and the integrations were performed on a 1024×1024 lattice.

In figure (1) we plot the imaginary part of the density response function, namely the spectral function, at zero temperature and $q = Q$. In curve (a) we show the spectral function calculated from the Self-consistent Linear Response theory, and show that the location of the peak agrees exactly with the value predicted by the exact theorem, indicated by a delta function arrow. The width of the peak is not intrinsic, but due to the finiteness of Γ used to smooth the calculations. In curve (b) we show the results from the usual RPA formula, and we see that it completely misses the location of the collective mode. For a larger value of U , this discrepancy becomes even stronger. In curve (c) we show the result of the simple BCS quasiparticle approximation to the density response function. It has an onset at the minimal value of $E_p + E_{p+Q} = 2|\mu|$, but no sharp peak structure of the collective mode.

In figures (2) and (3) we show the momentum dependence of the peak, by plotting the spectral function for various values of the center of mass momentum. It is interesting to note the difference in behaviour of the peak for different values of the interaction strength U . For the case of smaller U 's shown in Figure (2), we see that the collective mode is most sharply defined at $Q = (\pi, \pi)$, and that it broadens and disperses downwards in energy as one moves away from Q . For larger U 's, however, the energy of the mode increases as we go away from (π, π) with only a small change in the width or intensity of the peak. Within a simple T-matrix approximation of the η -mode, i.e. without the mixing into the density excitations, one can show that the η -mode always disperses downwards as one moves away from the (π, π) point, and it merges *tangentially* into the particle-particle continuum. The upward dispersion of the η -mode for large U can be attributed to the strong mixing of the η -mode with density excitations. We present a more detailed discussion of the dispersion of the mode and comparison between T-matrix approximation and the Self-consistent Linear Response method in Section V.

It is important to remind the reader that the special properties of the momentum Q demonstrated in figures above have nothing to do with the nesting property of the fermi surface, since we are studying a doped system where $2k_f$ is markedly different from Q at this filling. Instead, the special role of Q is that at this momentum, the η_q operator becomes an eigenoperator of the Hamiltonian. Physically speaking, this is the momentum where the particle-particle continuum vanishes.

In figure (4) we plot the temperature dependence of the spectral function for momentum Q . We see that the peak intensity decreases with temperature and the peak vanishes exactly at T_c . This behavior is in exact agreement with the third theorem that the peak intensity is proportional to the BCS order parameter. We also see that at low temperatures, the weight of the collective mode is transferred from the higher energy continuum.

FIGURES

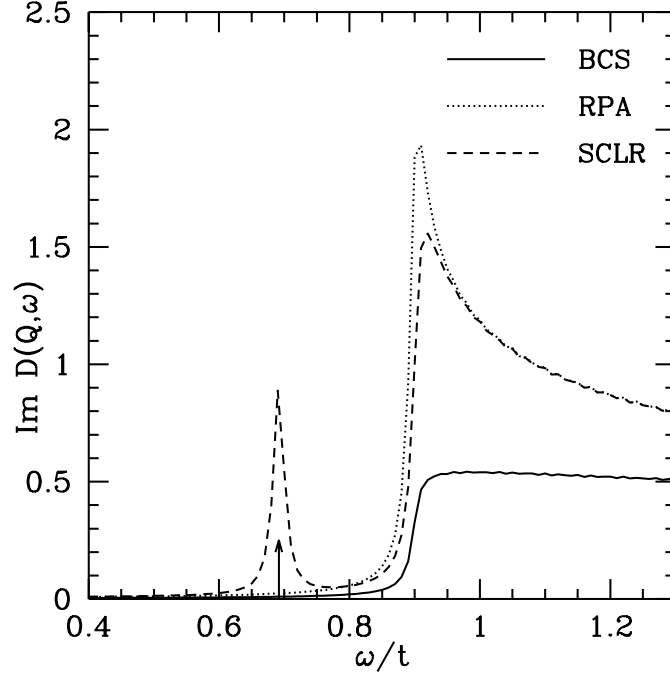


FIG. 1. $ImD(Q, \omega)$ versus ω calculated using BCS, Random Phase Approximation and Self-consistent Linear Response Theory formulas. The arrow indicates ω_0 - a position of the η -pair as predicted by the exact theorems. This plot is for $U = -t$, $n = 0.79$ and $T = 0$.

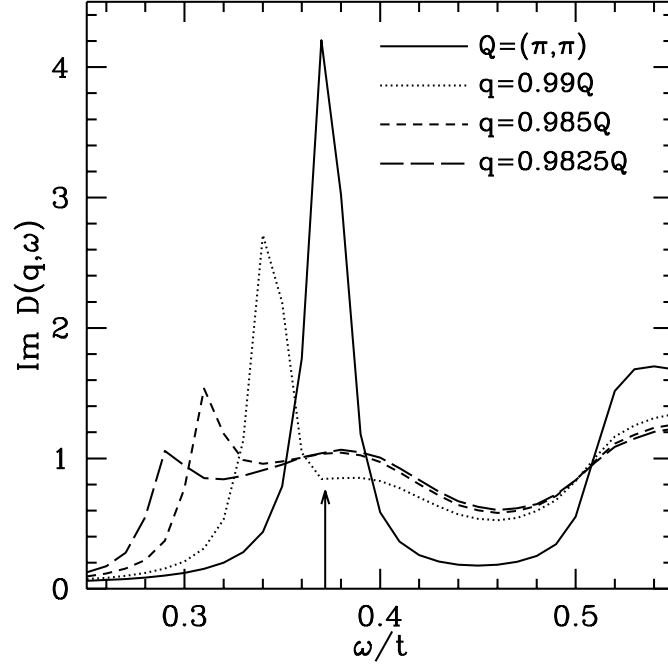


FIG. 2. $ImD(q, \omega)$ versus ω for $U = -t$, $n = 0.87$, $T = 0$ and different momenta q . The arrow marks ω_0 . This figure shows that for small U 's the collective η -mode exists only in a very close vicinity of (π, π) . One can also see a small dispersion of the mode - as we go away from (π, π) the energy decreases.

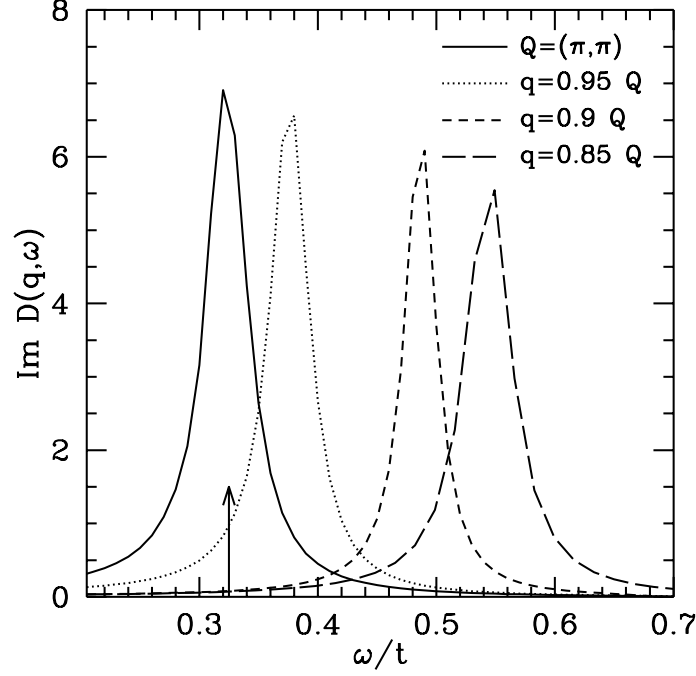


FIG. 3. $\text{Im} D(q, \omega)$ versus ω for $U = -4t$, $n = 0.87$, $T = 0$ and different momenta q . The arrow marks ω_0 . Notice a big positive dispersion and absence of strong damping of the mode away from (π, π) .

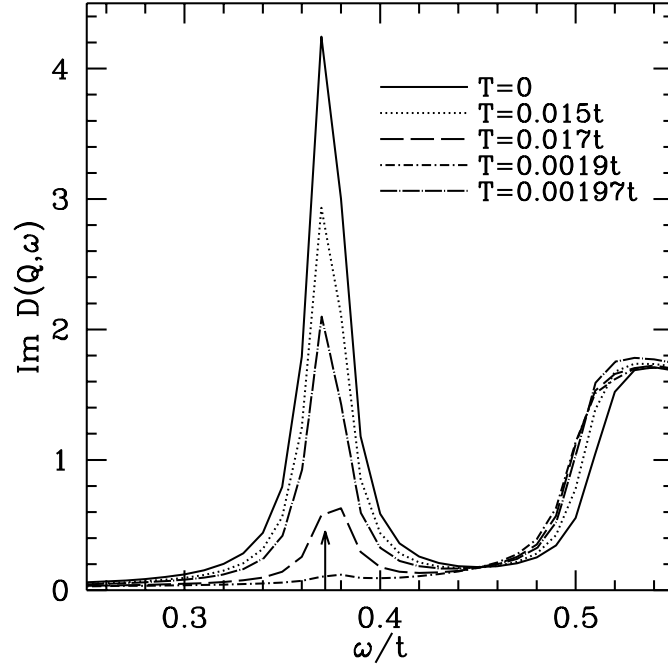


FIG. 4. $\text{Im} D(Q, \omega)$ versus ω for $U = -t$, $n = 0.87$ and different temperatures: $T = 0$ corresponds to $\Delta = 0.041t$; $T = 0.015t$ to $\Delta = 0.031t$; $T = 0.017t$ to $\Delta = 0.021t$; $T = 0.019t$ to $\Delta = 0.012t$ and $T = 0.0197t$ to $\Delta = 0.002t$. The arrow marks ω_0 . It is interesting that as we raise the temperature, the intensity of the peak decreases but its position does not change.

IV. MONTE CARLO CALCULATIONS

It is useful to compare the results of the exact theorems and the self-consistent calculations with the numerical data from Quantum Monte Carlo simulations. Using the finite-temperature determinantal Monte Carlo technique¹⁷ we have measured the Matsubara time-ordered Green's functions

$$D(q, \tau) = \langle T_\tau \rho_{-q}(\tau) \rho_q(0) \rangle \quad (41)$$

and

$$P(q, \tau) = \langle T_\tau \eta_q(\tau) \eta_q^\dagger(0) \rangle. \quad (42)$$

The spectral weights $\text{Im } D(q, \omega)$ and $\text{Im } P(q, \omega)$ can be obtained by maximum entropy analytic continuation^{18,19} of $D(q, \tau)$ and $P(q, \tau)$ to the real frequency axis.

In this section, we will present results for $U = -4t$ and $-1t$ on an 8×8 lattice. We will consider electron fillings $\langle n \rangle = 0.87, 0.7$ and 0.5 . For a filling of 0.87 and $U = -4t$, the Kosterlitz-Thouless superconducting transition temperature T_c^{KT} is $\simeq 0.1t$ ^{20,21}. In this parameter regime, we have carried out calculations for temperatures varying from $T = 0.5t$ down to $0.08t$.

The solid line in Fig. (5) shows $\text{Im } P(q, \omega)$ at center-of-mass momentum $q = (\pi, \pi)$ for $U = -4t$, $\langle n \rangle = 0.87$ and $T = 0.33t$. Here the chemical potential is $\mu = -2.15t$. We see that the peak is centered at $\omega_0 \simeq 0.37t$, which is close to $U - 2\mu$. The finite width of the peak is due to the resolution of the maximum entropy method. The dotted and the dashed curves in Fig. (5) show $\text{Im } P(q, \omega)$ for $q = (\pi, 3\pi/4)$ and $(3\pi/4, 3\pi/4)$. We observe that the η resonance broadens and shifts to higher frequencies as q moves away from (π, π) . The excitation is expected to disperse as $|q - (\pi, \pi)|^2$, however, the momentum resolution on the 8×8 lattice is $\pi/4$, and hence these calculations can't provide information on the dispersion of the η -resonance in the immediate vicinity of (π, π) .

Fig. (6) shows the spectral weight of the density response function, $\text{Im } D(q, \omega)$, at $q = (\pi, \pi)$ for various values of T . As the temperature is lowered a sharp peak develops at low frequencies. We note that the position of the peak in $\text{Im } D(q = (\pi, \pi), \omega)$ coincides with the position of the peak in $\text{Im } P(q = (\pi, \pi), \omega)$. In the grand canonical ensemble, the chemical potential depends on the temperature, and this is reflected in a slight shift of the peak position.

We can obtain further information on the density fluctuations by studying $D(q, \omega = 0)$. Fig. (7) shows $D(q, 0)$ versus q for q around the Brillouin zone at various temperatures. According to the Kramers-Kronig relation

$$D(q, 0) = \int_0^\infty \frac{d\omega'}{\pi} \frac{\text{Im } D(q, \omega')}{\omega'}, \quad (43)$$

$D(q, 0)$ provides us with information on the integral of the spectral weight divided by ω . In this figure we see that $D(q = (\pi, \pi), 0)$ increases rapidly as T is lowered. We believe that this rapid growth of $D(q = (\pi, \pi), 0)$ is due to the coupling of the density excitations to the η particle-particle channel as $T \rightarrow T_c^{\text{KT}}$. However, for $q \neq (\pi, \pi)$ such a rapid growth is not observed. This would then mean that the η excitation is relatively local in momentum space.

In Figure (6), we have seen that the peak in $\text{Im } D$ starts growing for temperatures considerably higher than T_c^{KT} . This is possibly due to the fact that there are significant superconducting fluctuations above T_c^{KT} . In order to obtain information on the strength of these superconducting fluctuations, we consider the current-current correlation function

$$\Lambda_{xx}(q, i\omega_m) = \frac{1}{N} \int_0^\beta d\tau e^{i\omega_m \tau} \langle j_x(q, \tau) j_x(-q, 0) \rangle \quad (44)$$

with

$$j_x(q) = it \sum_\ell e^{-iq \cdot \ell} (c_{\ell+x\sigma}^\dagger c_{\ell\sigma} - c_{\ell\sigma}^\dagger c_{\ell+x\sigma}). \quad (45)$$

The superfluid density D_s is given by²²

$$\frac{D_s}{\pi e^2} = -\langle k_x \rangle - \Lambda_{xx}(q_x = 0, q_y \rightarrow 0, i\omega_m = 0) \quad (46)$$

where $\langle k_x \rangle$ is the average kinetic energy in the x direction. In Fig. (8) we have plotted $-\langle k_x \rangle - \Lambda_{xx}(q_x = 0, q_y, i\omega_m = 0)$ versus q_y at various temperatures. These results, which are identical to those given in Fig. (8) of Ref.²², show that there are significant superconducting fluctuations on the 8×8 system for T higher than $T_c^{\text{KT}} \simeq 0.1t$. Basically the coherence length of the superconducting fluctuations is extending over the finite 8×8 lattice. We also note that the growth of D_s and the peak in $\text{Im } D$ appear to be strongly correlated, as one would have expected from the exact theorems of Section II.

For $U = -4t$ the statistical error in the Quantum Monte Carlo data is large, and as a result of this the spectral weights get smeared by the maximum entropy analytic continuation. For instance, in Fig. (5) we have seen that the η resonance, which is a δ function, was broadened considerably, and its frequency was shifted. However, for $U = -1t$ we can obtain Monte Carlo data with better statistics and the resulting spectral weights have improved resolution. Unfortunately, for $U = -1t$, the superconducting transition takes place at temperatures much lower than it is feasible for a numerical study. Hence, we will only study the η pair field susceptibility at the elevated temperature of $T = 0.25t$.

Here we consider the filling dependence of the η resonance. Fig. (9) shows $\text{Im } P(q = (\pi, \pi), \omega)$ versus ω/t for fillings of 0.87, 0.7 and 0.5. The corresponding chemical potentials are $-2.16t$, $-2.67t$ and $-3.25t$. We see from this figure that the resonance frequencies are very close to the expected values of $U - 2\mu$. In addition, we find that the total spectral weights in the peaks are 0.14, 0.31 and 0.49, respectively. These values agree well with the exact theorem of Eq. (8), which gives $1 - \langle n \rangle$ for the weight.

In this section, we have seen that a sharp resonance exists in the η -pairing channel. As the temperature is lowered and the superconducting correlations develop across the 8×8 lattice, the density fluctuations can couple to this channel. The resulting density excitation spectrum has a peak at the resonance frequency in addition to a continuum of excitations. These results are in agreement with the predictions of the exact theorems discussed in Section II and the results of the self-consistent calculations presented in Section III.

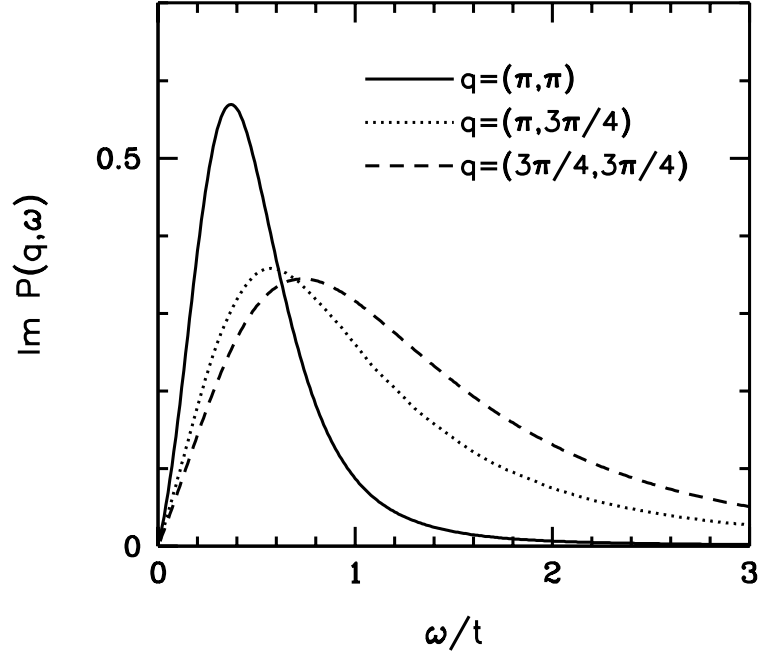


FIG. 5. $\text{Im } P(q, \omega)$ versus ω/t at various values of q for $U = -4t$, $\langle n \rangle = 0.87$ and $T = 0.33t$.

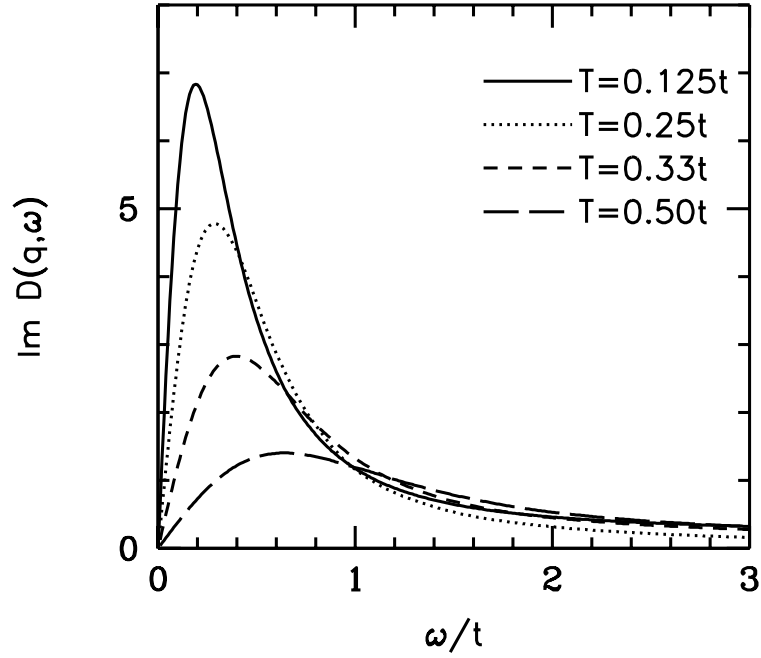


FIG. 6. $\text{Im } D(q = (\pi, \pi), \omega)$ versus ω/t for $U = -4t$, $\langle n \rangle = 0.87$ and various temperatures.

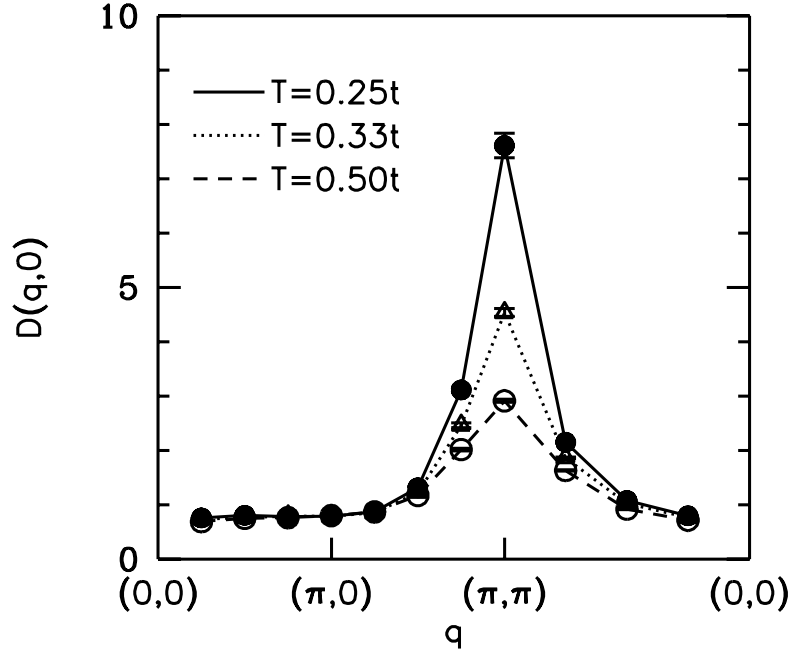


FIG. 7. $D(q, \omega = 0)$ versus q for $U = -4t$, $\langle n \rangle = 0.87$ and various temperatures.

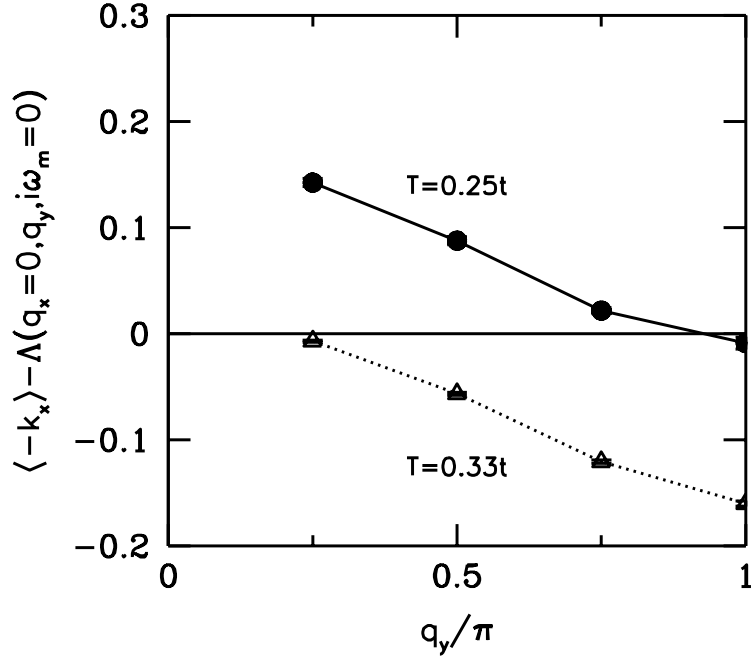


FIG. 8. $\langle -k_x \rangle - \Lambda_{xx}(q_x = 0, q_y, i\omega_m = 0)$ versus q_y/π for $U = -4t$, $\langle n \rangle = 0.87$ and various temperatures. The $q_y \rightarrow 0$ limit of this quantity gives the superfluid density, $D_s/\pi e^2$.

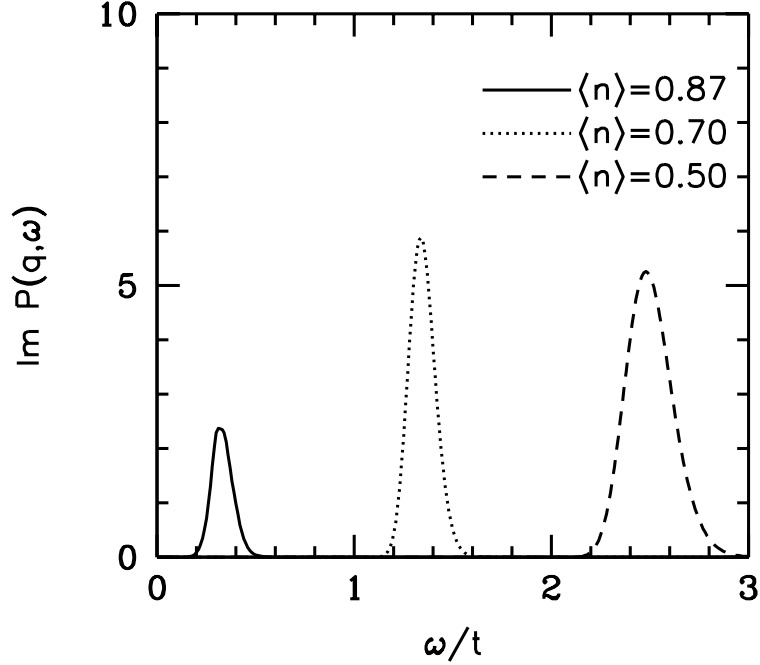


FIG. 9. $\text{Im } P(q = (\pi, \pi), \omega)$ versus ω/t for $U = -1t$, $T = 0.25t$ and various values of $\langle n \rangle$

V. MAPPING OF THE η -MODE TO ANTIFERROMAGNETIC SPIN WAVE

A. Particle-hole transformation

There is an elegant way to derive the dispersion of the η -mode for the negative U Hubbard model in the large $|U|$ limit by mapping it onto a Heisenberg model in an external magnetic field. Mele first used this formalism to discuss the dispersion of the η mode for zero temperature²³. Below we generalize this approach to include the effects of finite temperature and obtain the temperature dependence of the η mode dispersion.

Our starting point is a particle-hole transformation^{24,25,21} on the bipartite lattice:

$$\begin{aligned} c_{i\uparrow} &\rightarrow c_{i\uparrow} \\ c_{i\downarrow} &\rightarrow \begin{cases} +c_{i\downarrow}^\dagger, & i \in A \\ -c_{i\downarrow}^\dagger, & i \in B \end{cases} \end{aligned} \quad (47)$$

where A and B stands for the two sublattices. In the future we will write the transformation of the spin-down particles in the form $c_{i\downarrow} \rightarrow (-)^i c_{i\downarrow}^\dagger$.

For the two-fermion operators (47) gives

$$\begin{aligned} c_{i\uparrow}^\dagger c_{i\uparrow} &\rightarrow c_{i\uparrow}^\dagger c_{i\uparrow} \\ c_{i\downarrow}^\dagger c_{i\downarrow} &\rightarrow c_{i\downarrow} c_{i\downarrow}^\dagger = 1 - c_{i\downarrow}^\dagger c_{i\downarrow} \end{aligned} \quad (48)$$

and so the charge $Q = n_\uparrow + n_\downarrow$ becomes the spin $S_z = \frac{1}{2}(n_\uparrow - n_\downarrow)$ and vice versa.

$$Q \rightarrow 2S_z + 1 \quad 2S_z \rightarrow Q - 1 \quad (49)$$

If we now write our hamiltonian in the form

$$\mathcal{H} = -t \sum_{\langle ij \rangle \sigma} c_{i\sigma}^\dagger c_{j\sigma} - |U| \sum_i (n_{i\uparrow} - \frac{1}{2})(n_{i\downarrow} - \frac{1}{2}) - \tilde{\mu} \sum_{i\sigma} c_{i\sigma}^\dagger c_{i\sigma} \quad (50)$$

which is different from the earlier notation by only a chemical potential renormalization $\tilde{\mu} = \mu + \frac{|U|n}{2}$, we obtain using (48)

$$\mathcal{H} \rightarrow \mathcal{H} = -t \sum_{\langle ij \rangle \sigma} c_{i\sigma}^\dagger c_{j\sigma} + |U| \sum_i (n_{i\uparrow} - \frac{1}{2})(n_{i\downarrow} - \frac{1}{2}) - 2\tilde{\mu} \sum_{i\sigma} S_{iz} \quad (51)$$

Hamiltonian (51) describes a positive U Hubbard model at half-filling⁷ in the presence of a magnetic field $2\tilde{\mu}$ ⁸, which in the large U limit is known to be equivalent to the Heisenberg model

$$\mathcal{H} = J \sum_{\langle ij \rangle} \mathbf{S}_i \cdot \mathbf{S}_j - h \sum_i S_{iz} \quad (52)$$

with $J = \frac{4t^2}{U}$ and $h = 2\tilde{\mu}$. Therefore by considering the Heisenberg model, we will be able to get a deeper insight into the modes of the negative U Hubbard model.

Our next step will be to establish the correspondence between excitations of the two systems. To do so, we notice that the particle-hole transformation turns $SU(2)_{pseudospin}$ algebra into a usual $SU(2)_{spin}$ algebra

$$\begin{aligned} \eta^\dagger &= \sum_i (-)^i c_{i\uparrow}^\dagger c_{i\downarrow}^\dagger & \rightarrow & S_+ = \sum_i c_{i\uparrow}^\dagger c_{i\downarrow} \\ \eta &= \sum_i (-)^i c_{i\downarrow} c_{i\uparrow} & \rightarrow & S_- = \sum_i c_{i\downarrow}^\dagger c_{i\uparrow} \\ \eta_0 &= \frac{1}{2}(N_e - N) & \rightarrow & S_z = \frac{1}{2} \sum_i (c_{i\uparrow}^\dagger c_{i\uparrow} - c_{i\downarrow}^\dagger c_{i\downarrow}) \end{aligned} \quad (53)$$

And it transforms Cooper pairs and charge density wave into antiferromagnetic waves in $x - y$ and z directions respectively.

$$\begin{aligned} \Delta^\dagger &= \sum_i c_{i\uparrow}^\dagger c_{i\downarrow}^\dagger & \rightarrow & S_+(Q) = \sum_i (-)^i c_{i\uparrow}^\dagger c_{i\downarrow} \\ \Delta &= \sum_i c_{i\downarrow} c_{i\uparrow} & \rightarrow & S_-(Q) = \sum_i (-)^i c_{i\downarrow}^\dagger c_{i\uparrow} \\ \rho(Q) &= \sum_i (c_{i\uparrow}^\dagger c_{i\uparrow} + c_{i\downarrow}^\dagger c_{i\downarrow}) & \rightarrow & 2S_z(Q) = \sum_i (-)^i (c_{i\uparrow}^\dagger c_{i\uparrow} - c_{i\downarrow}^\dagger c_{i\downarrow}) \end{aligned} \quad (54)$$

⁷ We refer the reader to a well known theorem that $\mu = \frac{U}{2}$ at half-filling

⁸ Here and everywhere else we take Bohr's magneton to be one, $\mu_B = 1$.

Hamiltonian (52), as well as any other rotationally invariant system subject to an external magnetic field, has a Larmor precession mode given by

$$[\mathcal{H}, S_{\pm}] = \pm \hbar S_{\pm} \quad (55)$$

So, from (53) we see that η -excitation is what becomes of the Larmor motion under the particle-hole transformation.

Coupling of the η excitation to the density fluctuations also has its analogy in the Larmor motion. We assumed s -wave superconductivity in the negative U case, then after the particle-hole transformation takes us to the Heisenberg model we must have an antiferromagnetic order in $x-y$ plane or non-vanishing $\langle S_{\pm}(Q) \rangle$. The BCS order parameter being real implies that antiferromagnetism will be in x -direction. This means that $[S_{\pm}, S_z(Q)] = S_{\pm}(Q)$ is a c -number and so the Larmor motion is conjugate to the $S_z(Q)$ oscillations. Thus when we excite Larmor oscillations we will have a response in $S_z(Q)$. This is analogous to the negative U model in which η and CDW modes are conjugate $[\eta^{\dagger}, \rho(Q)] = \Delta^{\dagger}$ and therefore coupled to each other.

From the fact that the $\{\eta^{\dagger}, \eta, \rho(Q)\}$ operators for the negative U Hubbard model correspond to $\{S_+, S_-, S_z(Q)\}$ for the Heisenberg model, it follows that oscillations with wavevectors close to (π, π) will also be in one-to-one correspondence for the two systems and will therefore have the same dispersion. So in the next section we briefly review what is known regarding the excitations of the spin-wave modes of the Heisenberg Hamiltonian in an external magnetic field, Eq. (52).

B. Dispersion for the Heisenberg model

We consider a mean field spin-flop groundstate of the Hamiltonian, Eq. (52), which has antiferromagnetic order in the x -direction and is polarized in the z -direction by the magnetic field h so that

$$\langle \mathbf{S}_i \rangle = \frac{1}{2} \begin{pmatrix} (-)^i \alpha \\ 0 \\ \beta \end{pmatrix}. \quad (56)$$

As previously discussed, the antiferromagnetic order corresponds to the superconducting order in the negative U system and the magnetic polarization to the deviation of the band filling from half-filling. This means that temperature-wise $\alpha(T) \propto \Delta(T)$ and $\beta \propto 1 - n = \text{const.}$

If we now write the equations of motion for the individual spins

$$\frac{d\mathbf{S}_i}{dt} = i[\mathcal{H}, \mathbf{S}_i] \quad (57)$$

and linearize them around $\langle \mathbf{S}_i \rangle$ we get

$$\begin{aligned} \frac{d \delta S_i^x}{dt} &= \frac{J\beta}{2} \sum_{\langle j \rangle} [\delta S_j^y - \delta S_i^y] + h \delta S_i^y \\ \frac{d \delta S_i^y}{dt} &= (-)^i \frac{J\alpha}{2} \sum_{\langle j \rangle} [\delta S_j^z + \delta S_i^z] + \frac{J\beta}{2} \sum_{\langle j \rangle} [\delta S_i^x - \delta S_j^x] - h \delta S_i^x \\ \frac{d \delta S_i^z}{dt} &= (-)^i \frac{J\alpha}{2} \sum_{\langle j \rangle} [-\delta S_j^y - \delta S_i^y] \end{aligned} \quad (58)$$

where $\langle j \rangle$ stands for the sites nearest to i . We now take $M_i^z = (-)^i \delta S_i^z$ and $M_i^{x,y} = \delta S_i^{x,y}$, and perform a Fourier transformation of (58) to obtain

$$\begin{aligned} -i\omega M_{k\omega}^x &= -\frac{J\beta}{2}(4 - \gamma_k)M_{k\omega}^y + hM_{k\omega}^y \\ -i\omega M_{k\omega}^y &= \frac{J\alpha}{2}(4 - \gamma_k)M_{k\omega}^z + \frac{J\beta}{2}(4 - \gamma_k)M_{k\omega}^x - hM_{k\omega}^x \\ -i\omega M_{k\omega}^z &= -\frac{J\alpha}{2}(4 + \gamma_k)M_{k\omega}^y \end{aligned} \quad (59)$$

with $\gamma_k = \sum_{\mathbf{a}} e^{i\mathbf{k}\mathbf{a}}$. Equation (59) may be solved giving the dispersion relation²⁶

$$\omega_k^2 = \frac{J^2\alpha^2}{4}(16 - \gamma_k^2) + \left[\frac{\beta J}{2}(4 - \gamma_k) - h \right]^2 \quad (60)$$

For small k 's the last expression may be expanded to give

$$\omega_k^2 = h^2 + (2J^2\alpha^2 - h\beta J) \left[(k_x a)^2 + (k_y a)^2 \right] \quad (61)$$

Now we are in a position to discuss dispersion of the η -mode and compare the Self-consistent Linear Response with the T-matrix approximations. Above T_c , there is no mixing between the particle hole and the particle particle channels, a simple T-matrix calculation yields the correct answer of a downward dispersion. This result agrees with equation (61) when we take $\alpha^2 \propto |\Delta|^2 = 0$ above T_c . In the superconducting state a simple T-matrix approximation without taking into account the mixing is no longer valid. In fact, we see from (61) that the mixing term $2J^2\alpha^2$ gives a positive contribution to the dispersion. These two different terms compete with each other, so that a positive dispersion can be obtained at zero temperature for large $|U|$. On the other hand, for small $|U|$, the second term $-h\beta J$ always wins over the first term $2J^2\alpha^2$ and the dispersion is negative even at zero temperature. This is consistent with the numerical results of the Self-consistent Linear Response theory, presented in Section III C. From (61), we also see that at large $|U|$, as one rises the temperature from zero to T_c the temperature dependence of α leads to a continuous transition from the positive dispersion to negative.

VI. SUMMARY AND CONCLUSIONS

In this section we would like to summarize the results obtained in the previous sections, and comment on their implications. We see that the analytical approaches based on the $SO(4)$ symmetry property of the Hubbard model, the self-consistent linear response theory and the numerical Monte Carlo simulations agree with each other. These calculations establish that the η particle has the following properties:

- 1) It has charge quantum number two, and is a sharp excitation of the system for a finite range of total momentum around $Q = (\pi, \pi)$, and the mode disperses as the total momentum departs from Q . The special role played by Q is independent of the nesting property of the fermi surface.
- 2) It has spin zero and energy $U - 2\mu$.

3) Because it has charge two, it contributes to the particle-hole fluctuation spectrum (in this case the density spectrum) only when the superconducting pairing correlations are present. The analytic calculations show that the intensity of the peak onsets as the square of the superconducting order parameter. The energy of the peak is unchanged as a function of temperature.

The value of present detailed study of the η particle is to use it to illustrate a mechanism with which particle particle excitations can couple to the particle hole spectrum below T_c , and to test the methodology of the theoretical approach. We see that the Self-consistent Linear Response method correctly takes into account the contribution of the particle-particle excitation to the density fluctuation spectrum, and agrees with both the exact theorems derived from the $SO(4)$ Wards identities of the Hubbard model and the numerical Monte Carlo simulation results. This method is general, and thus provides a useful starting point for investigating the collective modes in the superconducting state.

In the next paper, we shall use the methodology developed and tested in this paper to carry out an investigation of the π particle of the positive U Hubbard or the $t - J$ model, which has spin one rather than zero, but shares many other properties of the η particle. We shall discuss in detail the similarities and differences of these two collective modes and compare our results with the neutron scattering experiments.

VII. ACKNOWLEDGMENTS

We would like to thank Prof. H. Fukuyama, R. Laughlin, J. R. Schrieffer and C.N. Yang for useful discussions. This work is supported by the NSF Materials Research Center at Stanford University. NB and DJS acknowledge support from the National Science Foundation under grant DMR92-25027. The computations were carried out at the San Diego Supercomputer Center.

VIII. APPENDIX A: COMPARISON WITH EQUATIONS OF MOTION METHOD

In the equations of motion method we introduce

$$\begin{aligned}\eta_{kq}^\dagger &= c_{k+q\uparrow}^\dagger c_{-k\downarrow}^\dagger \\ \eta_{kq} &= c_{-k-q\downarrow} c_{k\uparrow} \\ \rho_{kq} &= \rho_{kq\uparrow} + \rho_{kq\downarrow} = c_{k+q\uparrow}^\dagger c_{k\uparrow} + c_{-k\downarrow}^\dagger c_{-k-q\downarrow}\end{aligned}\tag{62}$$

and write the Heisenberg equations of motion for these operators using (13) as the Hamiltonian. These equations of motion are then factorized in terms of the occupation numbers for the electrons and BCS anomalous averages. The details of such computations are presented extensively in the literature^{4-6,8} and so we will only outline the main steps without going into details or discussing physical meaning of the equations.

$$\begin{aligned}[\mathcal{H}, \rho_{pq\uparrow}] &= \omega_{pq} \rho_{pq\uparrow} - (v_{p+q}^2 - v_p^2) U \left\{ \sum_k \rho_{kq\downarrow} + \frac{1}{2} \phi_q \right\} \\ &\quad + u_p v_p U \sum_k \eta_{kq}^\dagger - u_{p+q} v_{p+q} U \sum_k \eta_{kq} + \Delta (\eta_{pq}^\dagger - \eta_{pq})\end{aligned}\tag{63}$$

$$\begin{aligned}[\mathcal{H}, \rho_{pq\downarrow}] &= -\omega_{pq} \rho_{pq\downarrow} + (v_{p+q}^2 - v_p^2) U \left\{ \sum_k \rho_{kq\uparrow} + \frac{1}{2} \phi_q \right\} \\ &\quad + u_{p+q} v_{p+q} U \sum_k \eta_{kq}^\dagger - u_p v_p U \sum_k \eta_{kq} + \Delta (\eta_{pq}^\dagger - \eta_{pq})\end{aligned}\tag{64}$$

$$\begin{aligned}[\mathcal{H}, \eta_{pq}^\dagger] &= \Omega_{pq} \eta_{pq}^\dagger + U(1 - v_{p+q}^2 - v_p^2) \sum_k \eta_{kq}^\dagger \\ &\quad + U u_{p+q} v_{p+q} \left\{ \sum_k \rho_{kq\uparrow} + \frac{1}{2} \phi_q \right\} + U u_p v_p \left\{ \sum_k \rho_{kq\downarrow} + \frac{1}{2} \phi_q \right\} + \Delta (\rho_{pq\uparrow} + \rho_{pq\downarrow})\end{aligned}\tag{65}$$

$$\begin{aligned}[\mathcal{H}, \eta_{pq}] &= -\Omega_{pq} \eta_{pq} - U(1 - v_{p+q}^2 - v_p^2) \sum_k \eta_{kq} \\ &\quad - U u_{p+q} v_{p+q} \left\{ \sum_k \rho_{kq\uparrow} + \frac{1}{2} \phi_q \right\} - U u_p v_p \left\{ \sum_k \rho_{kq\downarrow} + \frac{1}{2} \phi_q \right\} - \Delta (\rho_{pq\uparrow} + \rho_{pq\downarrow})\end{aligned}\tag{66}$$

And we have already included the Hartree-Fock terms into the renormalized chemical potential. Following Anderson we take the second-order commutators

$$\begin{aligned}[\mathcal{H}, [\mathcal{H}, \eta_{pq} - \eta_{pq}^\dagger]] &= (\Omega_{pq}^2 + 4\Delta^2)(\eta_{pq} - \eta_{pq}^\dagger) - 2\Delta\omega_{pq}(\rho_{pq\uparrow} - \rho_{pq\downarrow}) \\ &\quad + U\Omega_{pq}(1 - v_{p+q}^2 - v_p^2) \sum_k (\eta_{kq} - \eta_{kq}^\dagger) \\ &\quad + 2U\Delta(u_p v_p + u_{p+q} v_{p+q}) \sum_k (\eta_{kq} - \eta_{kq}^\dagger) \\ &\quad - 2U\Delta(v_{p+q}^2 - v_p^2) \sum_k (\rho_{kq\uparrow} - \rho_{kq\downarrow}) \\ &\quad - U(u_p v_p + u_{p+q} v_{p+q}) \left[\mathcal{H}, \sum_k (\rho_{kq\uparrow} + \rho_{kq\downarrow}) \right]\end{aligned}$$

$$- U(1 - v_{p+q}^2 - v_p^2) \left[\mathcal{H}, \sum_k (\eta_{kq} + \eta_{kq}^\dagger) \right] \quad (67)$$

$$\begin{aligned} [\mathcal{H}, [\mathcal{H}, \eta_{pq} + \eta_{pq}^\dagger]] &= \Omega_{pq}^2 (\eta_{pq} + \eta_{pq}^\dagger) + 2\Delta\Omega_{pq} (\rho_{pq\uparrow} + \rho_{pq\downarrow}) \\ &+ U\Omega_{pq} (1 - v_{p+q}^2 - v_p^2) \sum_k (\eta_{kq} + \eta_{kq}^\dagger) \\ &+ U\Omega_{pq} (u_p v_p + u_{p+q} v_{p+q}) \left\{ \sum_k (\rho_{kq\uparrow} + \rho_{kq\downarrow}) + \phi_q \right\} \\ &- U(1 - v_{p+q}^2 - v_p^2) \left[\mathcal{H}, \sum_k (\eta_{kq} - \eta_{kq}^\dagger) \right] \end{aligned} \quad (68)$$

$$\begin{aligned} [\mathcal{H}, [\mathcal{H}, \rho_{pq\uparrow} - \rho_{pq\downarrow}]] &= \omega_{pq}^2 (\rho_{pq\uparrow} - \rho_{pq\downarrow}) - 2\Delta\omega_{pq} (\eta_{pq} - \eta_{pq}^\dagger) \\ &- U\omega_{pq} (u_p v_p + u_{p+q} v_{p+q}) \sum_k (\eta_{kq} - \eta_{kq}^\dagger) \\ &+ U\omega_{pq} (v_{p+q}^2 - v_p^2) \sum_k (\rho_{kq\uparrow} - \rho_{kq\downarrow}) \\ &- U(v_{p+q}^2 - v_p^2) \left[\mathcal{H}, \sum_k (\rho_{kq\uparrow} + \rho_{kq\downarrow}) \right] \\ &+ U(u_p v_p - u_{p+q} v_{p+q}) \left[\mathcal{H}, \sum_k (\eta_{kq} + \eta_{kq}^\dagger) \right] \end{aligned} \quad (69)$$

$$\begin{aligned} [\mathcal{H}, [\mathcal{H}, \rho_{pq\uparrow} + \rho_{pq\downarrow}]] &= (\omega_{pq}^2 + 4\Delta^2) (\rho_{pq\uparrow} + \rho_{pq\downarrow}) + 2\Delta\Omega_{pq} (\eta_{pq} + \eta_{pq}^\dagger) \\ &+ U\omega_{pq} (u_p v_p - u_{p+q} v_{p+q}) \sum_k (\eta_{kq} + \eta_{kq}^\dagger) \\ &+ 2\Delta U (1 - v_{p+q}^2 - v_p^2) \sum_k (\eta_{kq} + \eta_{kq}^\dagger) \\ &+ 2\Delta U (u_p v_p + u_{p+q} v_{p+q}) \left\{ \sum_k (\rho_{kq\uparrow} + \rho_{kq\downarrow}) + \phi_q \right\} \\ &+ U(v_{p+q}^2 - v_p^2) \left[\mathcal{H}, \sum_k (\rho_{kq\uparrow} - \rho_{kq\downarrow}) \right] \\ &- U(u_p v_p + u_{p+q} v_{p+q}) \left[\mathcal{H}, \sum_k (\eta_{kq} - \eta_{kq}^\dagger) \right] \end{aligned} \quad (70)$$

Now we take $[\mathcal{H}, f] = -\omega f$, where f can be any of ρ, η^\dagger or b , combine equations (67) with (69) and (68) with (70) such that unphysical poles $(\omega^2 - \theta_{pq}^2)$ cancel out and get after a few straightforward transformations:

$$\begin{aligned} (\omega^2 - \nu_{pq}^2) \rho_{pq} &= U\Omega_{pq} (u_p v_p + u_{p+q} v_{p+q}) \sum_k (\eta_{kq}^\dagger + \eta_{kq}) \\ &- U\omega (u_p v_p + u_{p+q} v_{p+q}) \sum_k (\eta_{kq}^\dagger - \eta_{kq}) \\ &+ U\nu_{pq} (v_p u_{p+q} + v_{p+q} u_p)^2 \left(\sum_k \rho_{kq} + \phi_q \right) \\ (\omega^2 - \nu_{pq}^2) (\eta_{pq}^\dagger + \eta_{pq}) &= U\Omega_{pq} (1 - v_{p+q}^2 - v_p^2) \sum_k (\eta_{kq}^\dagger + \eta_{kq}) \end{aligned} \quad (71)$$

$$\begin{aligned}
& - U\omega(1 - v_{p+q}^2 - v_p^2) \sum_k (\eta_{kq}^\dagger - \eta_{kq}) \\
& + U\Omega_{pq}(u_p v_p + u_{p+q} v_{p+q}) (\sum_k \rho_{kq} + \phi_q)
\end{aligned} \tag{72}$$

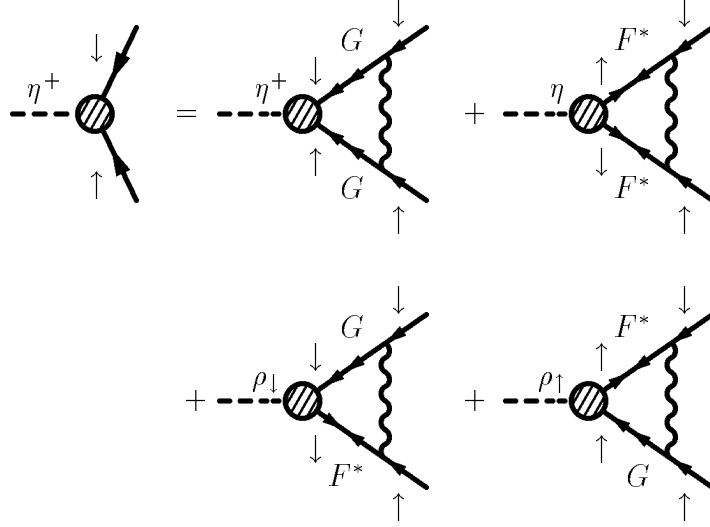
$$\begin{aligned}
(\omega^2 - \nu_{pq}^2) (\eta_{pq}^\dagger - \eta_{pq}) = & - U\omega(1 - v_{p+q}^2 - v_p^2) \sum_k (\eta_{kq}^\dagger + \eta_{kq}) \\
& + U\nu_{pq}(u_p u_{p+q} + v_p v_{p+q})^2 \sum_k (\eta_{kq}^\dagger - \eta_{kq}) \\
& - U\omega(u_p v_p + u_{p+q} v_{p+q}) (\sum_k \rho_{kq} + \phi_q)
\end{aligned} \tag{73}$$

One can see that after we divide equations (71) - (73) by $(\omega^2 - \nu_{pq}^2)$ and sum over p we recover the formulas of the Linear Response. The equations of motion method is very often more convenient because one gets equations before they were summed over momentum and this gives some additional freedom in manipulating them. So, for example it is much easier to see the η -pair energy-eigenvalue or to compute the residue of $D(q, \omega)$ at ω_0 in equations (71) - (73) than in (25) - (31). The same time the Linear Response Theory has an advantage of being more intuitively clear and transparent.

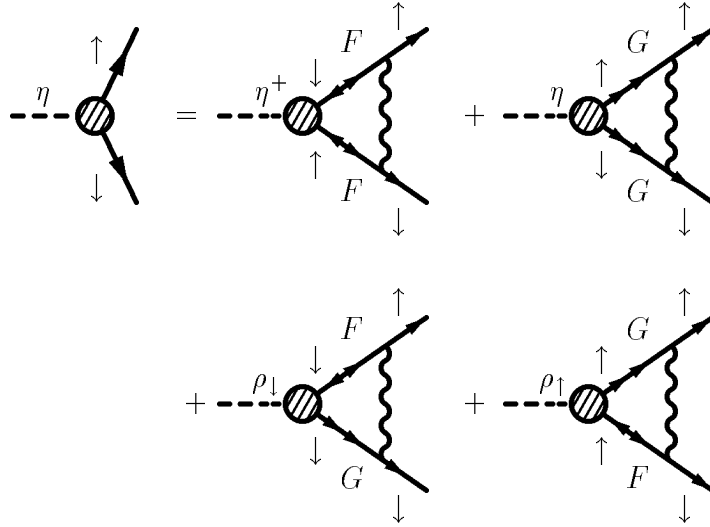
IX. APPENDIX B: DIAGRAMMATIC EQUATIONS

In this appendix we show the diagrams that correspond to equations (22) - (24).

The first equation describes scattering in the particle-particle channel and should be compared to (22).



This next equation is for scattering in the hole-hole channel and corresponds to (23).



The two following equations are for scattering in the particle-hole channels with spins up or down. Their sum gives (24).

Spin up:

$$\begin{aligned}
 & \text{Diagram 1: A dashed line labeled } \rho_{\uparrow} \text{ enters a shaded circle. Two solid lines exit the circle, both with upward arrows.} \\
 & = \text{Diagram 2: A dashed line labeled } \rho_{\uparrow}^0 \text{ enters a vertex. Two solid lines exit the vertex, both with upward arrows.} \\
 & + \text{Diagram 3: A dashed line labeled } \eta^+ \text{ enters a shaded circle. Two solid lines exit the circle, both with upward arrows. The circle is labeled } G \text{ (top) and } F \text{ (bottom).} \\
 & + \text{Diagram 4: A dashed line labeled } \eta \text{ enters a shaded circle. Two solid lines exit the circle, both with upward arrows. The circle is labeled } F^* \text{ (top) and } G \text{ (bottom).} \\
 & + \text{Diagram 5: A dashed line labeled } \rho_{\uparrow} \text{ enters a shaded circle. Two solid lines exit the circle, both with upward arrows. The circle is labeled } G \text{ (top) and } G \text{ (bottom).} \\
 & + \text{Diagram 6: A dashed line labeled } \rho_{\uparrow} \text{ enters a shaded circle. Two solid lines exit the circle, both with upward arrows. The circle is labeled } F^* \text{ (top) and } F \text{ (bottom).}
 \end{aligned}$$

Spin down:

$$\begin{aligned}
 & \text{Diagram 1: A dashed line labeled } \rho_{\downarrow} \text{ enters a shaded circle. Two solid lines exit the circle, both with downward arrows.} \\
 & = \text{Diagram 2: A dashed line labeled } \rho_{\downarrow}^0 \text{ enters a vertex. Two solid lines exit the vertex, both with downward arrows.} \\
 & + \text{Diagram 3: A dashed line labeled } \eta^+ \text{ enters a shaded circle. Two solid lines exit the circle, both with downward arrows. The circle is labeled } G \text{ (top) and } F \text{ (bottom).} \\
 & + \text{Diagram 4: A dashed line labeled } \eta \text{ enters a shaded circle. Two solid lines exit the circle, both with downward arrows. The circle is labeled } F^* \text{ (top) and } G \text{ (bottom).} \\
 & + \text{Diagram 5: A dashed line labeled } \rho_{\downarrow} \text{ enters a shaded circle. Two solid lines exit the circle, both with downward arrows. The circle is labeled } G \text{ (top) and } G \text{ (bottom).} \\
 & + \text{Diagram 6: A dashed line labeled } \rho_{\downarrow} \text{ enters a shaded circle. Two solid lines exit the circle, both with downward arrows. The circle is labeled } F^* \text{ (top) and } F \text{ (bottom).}
 \end{aligned}$$

REFERENCES

- ¹ C. Yang and S. Zhang, Modern Physics Letters B **4**, 759 (1990).
- ² S. Zhang, Phys. Rev. Lett. **65**, 120 (1990).
- ³ S. Zhang, International Journal of Modern Physics B **5**, 153 (1991).
- ⁴ P. Anderson, Phys. Rev. **112**, 1900 (1958).
- ⁵ G. Rickayzen, Phys. Rev. **115**, 795 (1959).
- ⁶ J. Schrieffer, *Theory of Superconductivity* (Benjamin/Cummings Publishing Co., Reading, Massachusetts, 1971).
- ⁷ A. Bardasis and J. Schrieffer, Phys. Rev. **116**, 235 (1987).
- ⁸ van der Marel, Phys. Rev. B **51**, 1147 (1995).
- ⁹ T. Kostyrko and R. Micnas, Phys. Rev. B **46**, 11 025 (1992).
- ¹⁰ J. Rossat-Mignod *et al.*, Physica C **185-189**, 86 (1991).
- ¹¹ J. Rossat-Mignod *et al.*, Physica C **235-240**, 1687 (1994).
- ¹² H. Mook *et al.*, Phys. Rev. Lett. **70**, 3490 (1994).
- ¹³ H. F. Fong *et al.*, Phys. Rev. Lett. **75**, 316 (1995).
- ¹⁴ E. Demler and S. Zhang, Phys. Rev. Lett. **75**, 4126 (1995).
- ¹⁵ C. Yang, Phys. Rev. Lett. **63**, 2144 (1989).
- ¹⁶ K. Machida, K. Nokura, and T. Matsubara, Phys. Rev. Lett. **44**, 821 (1980).
- ¹⁷ S. White *et al.*, Phys. Rev. B **40**, 506 (1989).
- ¹⁸ R. Silver, D. Sivia, and J. Gubernatis, Phys. Rev. B **41**, 2380 (1990).
- ¹⁹ S. White, Phys. Rev. B **41**, 2380 (1990).
- ²⁰ R. Scalettar *et al.*, Phys. Rev. Lett. **62**, 1407 (1989).
- ²¹ A. Moreo and D. Scalapino, Phys. Rev. Lett. **66**, 946 (1991).
- ²² D. Scalapino, S. White, and S. Zhang, Phys. Rev. B **47**, 7995 (1993).
- ²³ E. Mele, Solid State Communications **79**, 515 (1991).
- ²⁴ H. Shiba, Prog. Theor. Phys **48**, 2171 (1971).
- ²⁵ J. E. Hirsch, Phys. Rev. B **31**, 4403 (1985).
- ²⁶ R. M. White, *Quantum Theory of Magnetism* (McGraw-Hill, New York, 1970).